A Letters Journal Exploring the Frontiers of Physics

December 2019

EPL, **128** (2019) 60002
doi: 10.1209/0295-5075/128/60002

www.epljournal.org

Information retrieval from modified Kuramoto network by resonant synchronization

Xu Li, Tingting Xue and Lin Zhang[(a)]

School of Physics and Information Technology, Shaanxi Normal University - Xi'an 710061, PRC

received 9 July 2019; accepted in final form 3 January 2020
published online 4 February 2020

PACS 05.45.Xt – Synchronization; coupled oscillators
PACS 05.45.-a – Nonlinear dynamics and chaos

Abstract – A collective behavior of resonant synchronization (RS) in an inhomogeneous network is investigated and its function to retrieve information from encoding networks is proposed based on the RS mechanism. We use modified Kuramoto phase oscillators to simulate normal neurons in self-oscillation state, and investigate the collective responses of a fully connected neuronal network to the stimulus signals when the network is in a critical state just below the synchronization threshold. The stimulus driving on one node at resonant frequencies can stimulate the unsynchronized rotators across the network into collective synchronized states locked to similar frequencies, and thus recover the memorized locations through the synchronized patterns related to the predetermined frequency distributions among the oscillators. This model suggests a potential mechanism to explain how brain stores and retrieves information from resonant synchronization patterns emerging from an inhomogeneous critical neuronal network stimulated by the resonant external driving.

Introduction. – The consciousness of human brain and its memory mechanism are the most fascinating problems in physics and biology [1–3]. With the help of molecular biology and brain magnetic resonance imaging (MRI), neurobiologists have identified some physical structures and collective dynamics of neurons in certain functional regions [4]. The cerebral cortex has proved to be a complex network of well-connected neurons working in a critical state which can exhibit synchronized behaviors of neuron firings induced by certain stimulus sources [5].

As synchronized patterns of neurons are involved in the cognitive activities, different mathematical models were proposed to understand the consciousness activities at different space-time scales [6–8]. However, due to the complexity of neuronal network, the collective behavior (whole-brain dynamics) remains unclear and no efficient analytical analysis is available on these multi-agent systems. Most dynamical simulations are limited to give macroscopic properties of steady-state behaviors [9] or the aberrant dynamics of neural activities [10]. Based on the synchronized spatiotemporal patterns emerged in the large-scale brain activities [11], we adopt the Kuramoto network model [12,13], a typical microscopic model of globally coupled nonlinear rotators, to study the collective dynamics of neutrons working in self-sustained states when a driving force is introduced. Many similar works have been done to investigate the perturbation spreading [14] and the pinning control [15] of the network with continuous harmonic driving. However, our study focuses on another aspect of driving problem and finds that the Kuramoto network presents an enhanced synchronization that can be explored to fulfill information retrieval from an inhomogeneous critical network by resonant stimulations [16–20]. By studying the synchronization of the Kuramoto network with Pearson correlation coefficient, we find that when the coupling strength between Kuramoto oscillators (KOs) is just below the synchronization threshold, the globally coupled KOs will synchronize even ONE node of the network which is driven by a resonant external driving. What we found in this paper probably suggests a potential mechanism of memory encoding and retrieval in a well-connected critical network with a resonant driving scheme.

The resonant synchronization. –

Resonant synchronization in Kuramoto network. After Huygens' first observation of synchronized motion between two adjacent pendulum clocks in 1673,

[(a)]E-mail: zhanglincn@snnu.edu.cn

synchronization was proved to be a universal phenomenon in nature and has been extensively studied in many fields [21,22]. In recent years, the synchronized behaviors of neural activities have received widespread attention and many physical models are proposed [23–30]. Here, we adopt the Kuramoto model to study the resonant synchronization effect and apply it to the memorized dynamics of neuronal network. The Kuramoto model describes globally coupled phase oscillators which exhibit synchronization behaviors when the coupling rate k reaches a critical value k_c [12,31]. In a two-node Kuramoto network, the dynamical equations are

$$\dot{\theta}_1 = \omega_1 + \frac{k}{2}\sin(\theta_2 - \theta_1) + \hat{\xi}_1(t), \tag{1}$$

$$\dot{\theta}_2 = \omega_2 + \frac{k}{2}\sin(\theta_1 - \theta_2) + \hat{\xi}_2(t), \tag{2}$$

where each oscillator has its own eigenfrequency ω_1 or ω_2, and k is their coupling rate. These equations can describe two neutrons in their limit-cycle states with spiking phase θ_i in a noisy background described by noise operator $\hat{\xi}_i(t)$. Then the relative spiking phase between two rotators is

$$\dot{\delta\theta} = \delta\omega - k\sin(\delta\theta) + \delta\hat{\xi}(t), \tag{3}$$

where $\delta\theta = \theta_2 - \theta_1$, $\delta\omega = \omega_2 - \omega_1$ and $\delta\hat{\xi}(t) = \hat{\xi}_2(t) - \hat{\xi}_1(t)$. Here, we suppose a common white noise background with a zero time-average mean-field effect of $\langle\delta\hat{\xi}(t)\rangle \approx 0$ due to $\hat{\xi}_1(t) = \hat{\xi}_2(t) = \hat{\xi}(t)$ with $\langle\hat{\xi}(t)\hat{\xi}(t')\rangle = \eta\delta(t - t')$, and we introduce a weak noise strength η in our simulations.

As eq. (3) gives a synchronized condition of $k \geq |\delta\omega|$, two direct ways are feasible to synchronization: increasing coupling strength k and decreasing frequency deviation $\delta\omega$. Here, we introduce external driving instead to simulate network synchronization because mental activities (*e.g.*, imagination or thinking) are always triggered by successive signals of certain stimulations. Then the full equations become [14]

$$\dot{\theta}_1 = \omega_1 + \frac{k}{2}\sin(\theta_2 - \theta_1) + \Lambda\sin(\Omega t - \theta_1) + \hat{\xi}(t), \tag{4}$$

$$\dot{\theta}_2 = \omega_2 + \frac{k}{2}\sin(\theta_1 - \theta_2) + \hat{\xi}(t), \tag{5}$$

where Λ is the driving strength, Ω the driving frequency and $\hat{\xi}(t)$ the common background noise. In this case the dynamics of the relative spiking phase will be

$$\dot{\delta\theta} = \delta\omega - k\sin\delta\theta - \Lambda\sin(\Omega t - \theta_1) + \delta\hat{\xi}(t), \tag{6}$$

where the noise $\delta\hat{\xi}(t)$ can be neglected for a mean-field analysis. Obviously, if the driving frequency Ω is far-off detuned from any KOs, namely $\Omega \gg \omega_i$, the contribution of the driving term on the right-hand side of eq. (6) will disappear for $\int\sin(\Omega t - \theta_1)dt \approx 0$. Conversely, if Ω is resonant with rotator 1, that is, $\Omega \sim \omega_1$, then eq. (6) goes to eq. (3) due to $\Omega t \approx \theta_1$ for a small k, and k_c changes

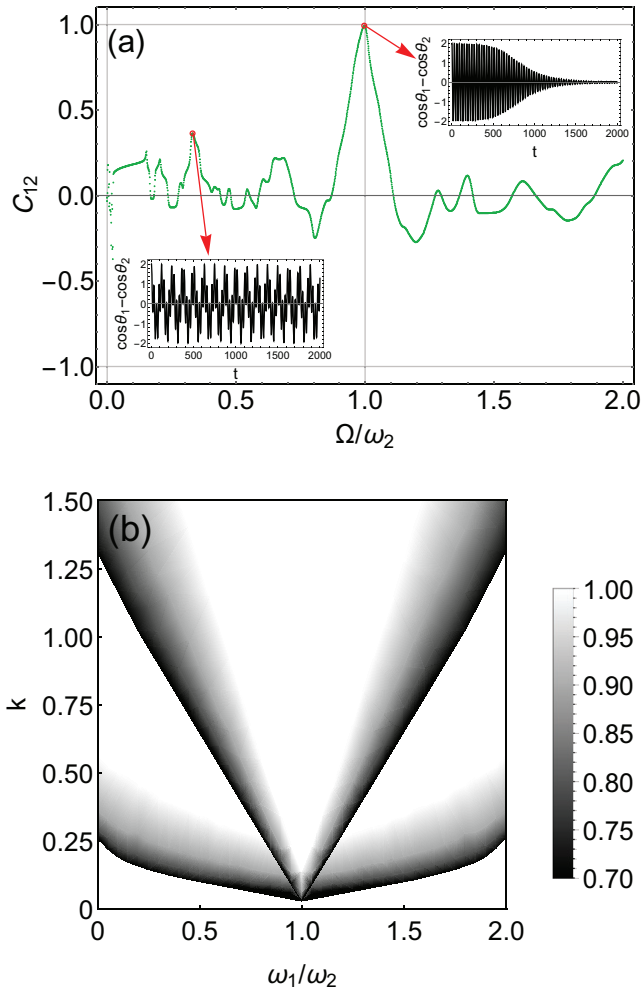

Fig. 1: (a) The synchronization degree estimated by a long-time analysis of C_{12} varies with respect to the external driving frequency Ω. The eigenfrequencies of two rotators are $\omega_1 = 0.2, \omega_2 = 0.21$, and the coupling strength $k = 0.008$. Inset: the relative phases of two rotators estimated by $\cos\theta_1 - \cos\theta_2$ sampled at driving frequencies of $\Omega/\omega_1 = 0.35$ and $\Omega/\omega_1 = 1$. (b) Arnold tongue describing the synchronization region estimated by C_{12}. The upper tongue area represents the synchronization without external driving, and the lower one is for the case by adding the external driving with $\Lambda = 1$, $\Omega = 0.2$ and noise strength of $\eta = 0.01$.

a little. While if the driving frequency adjusts to $\Omega \sim \omega_2$ and $\Omega t \sim \theta_2$, eq. (6) becomes

$$\dot{\delta\theta} \approx \delta\omega - (k + \Lambda)\sin\delta\theta, \tag{7}$$

which clearly gives a new critical coupling rate $k_c' \equiv k_c - \Lambda < k_c$ under an in-phase resonant driving for $\Lambda > 0$. Therefore, keeping the coupling rate k below the synchronization threshold k_c, *i.e.*, the system is initially in a nonsynchronous state, the oscillators will synchronize by adding an external signal with a driving frequency close to the eigenfrequencies of coupled rotators.

In fig. 1(a) we directly simulate this resonant synchronization behavior through Pearson correlation coefficient

$C_{12}(t)$ after a long time evolution. We calculate the correlation of $C_{12}(t)$ in a time window of $\Delta t > 1/\min(\omega_i)$ for a dynamical measure to estimate the degree of synchronization between rotators 1 and 2. When two KOs are completely synchronized or anti-synchronized, the coefficient C will be 1 or -1 [32]. Figure 1(b) clearly shows that when the driving frequency is tuned near to their eigenfrequencies, the system achieves an enhanced synchronization with a weaker coupling $k < k_c$. In order to identify this resonant synchronization effect, the Arnold tongues of synchronization are calculated in fig. 1(b) with respect to the coupling rate k and the frequency ratio ω_1/ω_2. We can see a clear decrease of critical coupling of k_c for resonant synchronization and an increase of synchronous area by introducing the resonant driving.

Generally, a well-connected local network can be simulated by a group of N all-to-all coupled Kuramoto oscillators (KOs) and each of them can be described by a complex wave function

$$\psi_l(t) = e^{i\theta_l(t)}, \quad l = 1, 2, \ldots, N. \tag{8}$$

The phases of the wave functions are governed by

$$\dot{\theta}_l = \omega_l + \frac{k}{N}\sum_{j=1}^{N}\sin(\theta_j - \theta_l) + \hat{\xi}(t). \tag{9}$$

In order to study the collective dynamics of KOs, a collective wave packet is often introduced

$$\Psi(t) = \frac{1}{N}\sum_{j=1}^{N}\psi_j(t) \equiv r(t)e^{i\phi(t)}, \tag{10}$$

which is a superposition of all the wave functions ψ_j, and $r(t)$ and $\phi(t)$ are the amplitude and phase functions of the wave packet, respectively. Substituting eq. (10) into eq. (9), we have

$$\dot{\theta}_l = \omega_l + kr\sin(\phi - \theta_l) + \hat{\xi}(t). \tag{11}$$

Therefore, we define the relative phases $\theta'_l = \theta_l - \phi$ and the group phase of the wave packet satisfies a mean-field equation

$$\frac{\mathrm{d}\phi}{\mathrm{d}t} = \overline{\omega}, \tag{12}$$

where $\overline{\omega}$ is the group frequency of the wave packet determined by the average frequency of all the wave components

$$\overline{\omega} = \frac{1}{N}\sum_{j=1}^{N}\frac{\mathrm{d}\theta_j}{\mathrm{d}t}. \tag{13}$$

In this case, eq. (11) becomes

$$\dot{\theta}'_l = (\omega_l - \overline{\omega}) - kr\sin\theta'_l, \tag{14}$$

where we neglect the phase noises for a mean-time dynamical analysis. When the phase locking of KOs occurs, the relative phases must be $\dot{\theta}'_l \approx 0$ and eq. (14) leads to

$$\sin\theta'_l \approx \frac{\omega_l - \overline{\omega}}{kr}, \tag{15}$$

that is

$$\left|\frac{\omega_l - \overline{\omega}}{kr}\right| \leq 1. \tag{16}$$

Therefore, the condition of a synchronized state for KOs requires that the frequency deviations of the oscillators meet

$$-|kr| \leq \omega_l - \overline{\omega} \leq |kr|. \tag{17}$$

Now, if we introduce an external driving to one of the oscillators α in the cluster of KOs, the dynamical equation for the oscillator α will be

$$\dot{\theta}_\alpha = \omega_\alpha + kr\sin(\phi - \theta_\alpha) + \Lambda\sin(\Omega t - \theta_\alpha) + \hat{\xi}(t). \tag{18}$$

For a resonant driving on oscillator α for $\Omega \approx \overline{\omega}$, a similar derivation based on eq. (11) can give the synchronization condition of the α oscillator to the group as

$$-|kr + \Lambda| \leq \omega_\alpha - \overline{\omega} \leq +|kr + \Lambda|. \tag{19}$$

Comparing eq. (19) with eq. (17), it is easy to find that the occurrence of phase locking for a resonant-driven oscillator ($\Lambda > 0$ for in-phase driving) is more relaxed to the frequency requirement for cluster synchronization. With the all-to-all mutual couplings, a robust local driving will easily transmit throughout a well-connected critical network by resonant activation and all the KOs with similar frequencies in the group will be dynamically synchronized with each other. In other words, the synchronization becomes easier when a resonant driving is introduced to a critical network just below synchronization threshold of KOs, and, consequently, the synchronization will be enhanced by a positive feedback of eq. (19), establishing an enhanced coherent motion under the resonant effect. As the strength of noise only shifts the critical coupling rate k_c [31], direct simulations prove that the resonant synchronized effects are immutable to noises in a critical network if the resonant driving is strong enough.

Resonant synchronization and synchronized groups selected by resonant driving. Now, we apply the above resonant synchronization effect to information retrievals in our brain's neural network. The brain neural system is composed of nearly 86 billion of mutually coupled neurons [33], where dendrites or axons of neurons connect with each other through synapses to form a high-degree connected neuronal network [34]. By passing electrochemical signals through synapses between neurons, the neurons can be excited or inhibited which makes the neuron spiking in the cortical system exactly a discontinuous nonlinear process [35]. The human brain is a complicated multiscale network [36], and thus impossible to reveal its functionality by just resolving the structures and the dynamics of individual neurons, but should include all the connected neurons as a whole dynamical system.

As the conventional Kuramoto model excludes the influence of brain environments and cannot be directly applied to a neuronal network, we modify the Kuramoto model

by including the variations of the frequencies and the coupling strengths of KOs to describe a critical dynamics of neurons [16]. Due to the chemical changes of synapses or the neurotransmitter diffusion, the coupling strength between neurons and the neuron spiking frequency (or firing rate) will change over time under stimuli and the large time scale variations (long-time memory) are excluded here. Therefore, the spiking frequencies and the coupling strengths of neurons are dominated by a constant part plus a weak sinusoidal modulation. Hence, the modified Kuramoto model will be

$$\dot{\theta}_i = \omega_i(t) + \frac{1}{N}\sum_{j=1}^{N} k_{ij}(t)\sin(\theta_j - \theta_i) + \hat{\xi}(t), \qquad (20)$$

where $\omega_i(t)$ and $k_{ij}(t)$ are the time-varying frequencies of neuron i and the coupling strengths between neurons i and j, respectively, which are supposed to be governed by the following simple time-dependent functions:

$$\omega_i(t) = \omega_i + \beta_i \sin(2\pi f_i t + \varphi_i), \qquad (21)$$

$$k_{ij}(t) = k_{ij} + \mu_{ij}\sin(2\pi g_{ij} t + \psi_{ij}), \qquad (22)$$

where the constants ω_i and k_{ij} are the long-time eigenfrequencies and coupling strengths to define a basic critical network. The modulation parameters $\beta_i = 0.1\omega_i$, $\mu_{ij} = 0.1k_{ij}$, $f_i = 1$, $g_{ij} = 0.3$, $\varphi_i = \pi/2$ and $\psi_{ij} = \pi$ describe the amplitudes, frequencies and phase offsets of the time-varying parts [16]. When the system is near to the coupling thresholds $k < k_c$, we study the dynamical synchronization between neurons when an external driving is added to one of KOs. In order to simulate information retrieval from memory in a critical brain state that the neuron firings are continuously activated by successive stimuli, we introduce an activated driving signal of sinusoidal mode $\Lambda\sin(\Omega t - \theta_l)$, acting on lth KO (an oscillator selected in certain regions), then the equation of the driven oscillator becomes:

$$\dot{\theta}_l = \omega_l(t) + \frac{1}{N}\sum_{j=1}^{N} k_{lj}(t)\sin(\theta_j - \theta_l) + \Lambda\sin(\Omega t - \theta_l). \qquad (23)$$

Figure 2 simulates a globally coupled network with a number of $N = 12$ KOs starting from random initial phases and demonstrates a clear phase bunching after adding an external driving signal. When the driving is added to any one oscillator of the network, the oscillators whose eigenfrequencies ω_i are close to the driving frequency Ω will synchronize their motions to a synchronization state and then the phase bunching appears. The solid circles shown in fig. 2(b) demonstrate a synchronized KO cluster, moving around together with a group angular velocity $\overline{\omega}$ under the external resonant driving.

In order to show the details of the resonant synchronization, we consider $N = 6$ KOs and analyze the synchronization dynamics of these coupled KOs. In this small

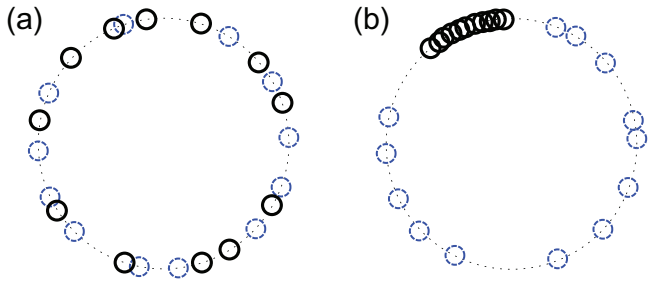

Fig. 2: Phase distributions of θ_i for $N = 12$ KOs shown on a unit circle (a) without and (b) with the external driving after a same period of evolution. The dashed circles denote the initial phase distributions of KOs and the solid ones are the phase distributions after $t = 2000$. The frequencies ω_i of the KOs are randomly sampled between the interval of $[0.9, 1.1]$, the driving parameters are $\Lambda = 1, \Omega = 1$ and the coupling rate $k_{ij} = 1 < k_c$.

network, we initially set the eigenfrequencies of oscillators 1, 3, 5 randomly around 1.0, and 2, 4, 6 around 2.0 with small deviations (see the parameters in fig. 3). Here, the eigenfrequencies set in advance stand for the stored information in the neurons which is characterized by its firing eigenfrequency ω_i. When an external signal with a driving frequency of $\Omega = \omega_1$ is added to one node of the KO network (see the bottom left inset of fig. 3), the oscillators $1, 3$ and 5 synchronize into a group with enhanced mutual Pearson correlation coefficients shown in fig. 3 (see the resonant peaks of curves C_{13}, C_{15} and C_{35}). If the driving frequency changes to $\Omega = 2\omega_1$ (see the bottom right inset of fig. 3), the KOs of 2, 4 and 6 are synchronized instead (see the resonant peaks of curves C_{24}, C_{26} and C_{46}) due to the resonant properties of the synchronization selected by external stimuli of different driving frequencies.

The pattern retrieved from the memorized lattice network by resonant synchronization. Now, we will show how to use the resonant synchronization to recover stored images in a well-connected network of KOs. In order to reveal its mechanism, we investigate the synchronized behaviors of neurons in a regular neuronal network induced by external driving sources based on the above-modified Kuramoto model equation (20). We use a globally coupled neural network of 20×20 KO lattice to simulate the well-connected neurons in a local area of cerebral cortex in our brain. Here, the eigenfrequencies are used to encode the information in the neural network. We set the eigenfrequencies of the coded KOs in advance by a Gaussian distribution with the same mean value ω_0 to construct an image of "5" through a spatial configuration in the lattice network, and the eigenfrequencies of the other uncoded KOs are assigned randomly. When the lattice network is subjected to an external stimulus with a driving frequency of Ω, the neurons with eigenfrequencies near to Ω are activated and then synchronized together by the continuous resonant driving. All the KOs with enhanced C_{ij} recover a synchronized pattern of "5" emerging in the

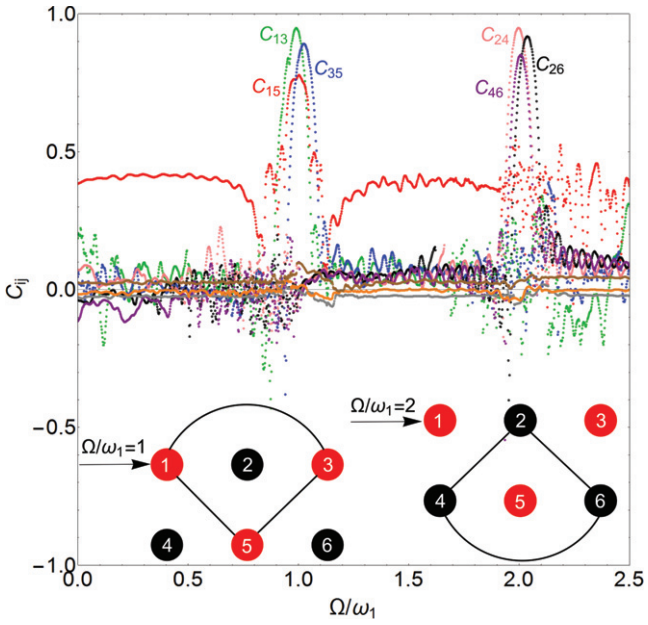

Fig. 3: The resonant synchronization of $N = 6$ KOs estimated by C_{ij} *vs.* the driving frequency Ω. The eigenfrequencies of the oscillators are $\omega_1 = 0.94$, $\omega_3 = 1$, $\omega_5 = 1.06$, $\omega_2 = 1.97$, $\omega_4 = 2$, $\omega_6 = 2.03$, respectively. The coupling, driving and noise strengths are $k_{ij} = 0.36$, $\Lambda = 1$ and $\eta = 0.01$, respectively. Two different driving frequencies are $\Omega/\omega_1 = 1$ and $\Omega/\omega_1 = 2$. Insets: the networks of 6 KOs driven by external signals with frequencies of Ω_1 (left) and Ω_2 (right), the synchronized KOs are connected by the solid lines.

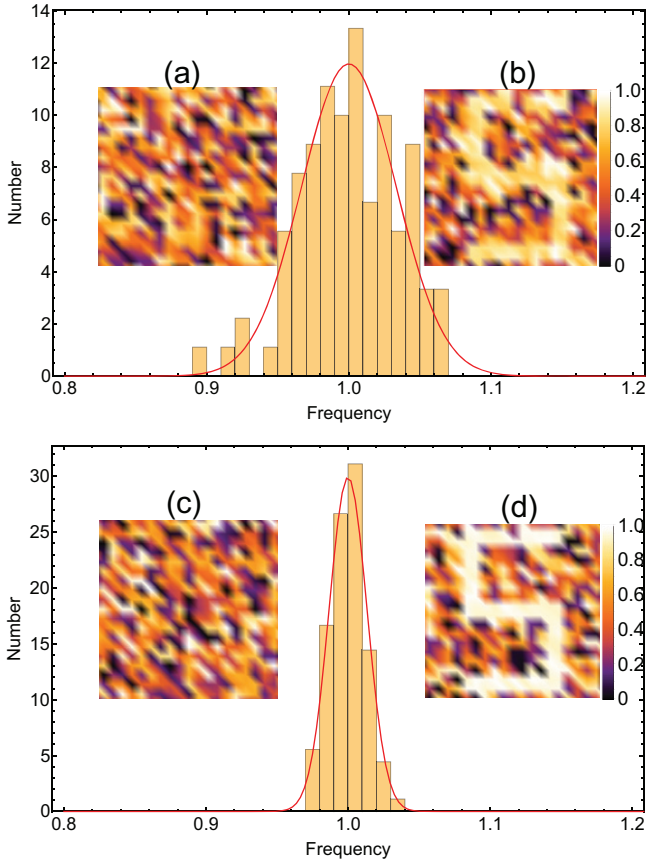

Fig. 4: Synchronization pattern retrievals from C_{ij} without external driving ((a), (c)) and with resonant driving ((b), (d)). The frequencies of the memorized KOs are assigned by Gaussian distributions with mean value of $\omega_0 = 1$ and the deviations of 0.1/3 (the upper frame) and 0.04/3 (the lower frame), the frequencies of other KOs are set randomly from the interval [0, 2]. The resonant driving strength $\Lambda = 1$ and the coupling rate $k_{ij} = 1.36$. The other parameters are the same as in fig. 3.

network as shown in fig. 4. The images in the left column, fig. 4(a), (c), are displayed by the mutual synchronous matrix of C_{ij} without adding stimulus signals, while the images in the right column, fig. 4(b), (d), are C_{ij} under the stimulus of $\Omega = \omega_0 = 1$. When we add the driving signal to the network, the active pattern appears so that KOs with the similar stored eigenfrequencies are activated and synchronized together by the resonant driving (right column). If there is no input signal, all KOs oscillate weakly with their own eigenfrequencies and the dynamics of the whole network is in a random state. In this case, the network are not synchronized and no synchronized pattern will be produced (left column). We can numerically verify that this retrieval process is robust to noise because the network is in a critical state just below the synchronization threshold ($k_c = 1.42$ for a free KO model) and the critical dynamics is sensitive to the driving signals. Therefore, by direct simulations, we find a sychronized pattern emergence in a frequency coding network if a resonant external stimulus is introduced.

Considering that memory is a very complex process with a large number of randomly arranged neurons in a noisy background, the dynamics of neurons in human brain may not as simple as that we considered above, but this simplified model can still provide us with a possible idea of memory searching mechanism in the brain. In order to simulate different intensities of unavoidable memory deviations in the network, we encode KOs' eigenfrequencies with Gaussian distributions of different deviations. The direct simulations find that the resonant synchronous patterns of C_{ij} are recovered in different resolutions by the same intensity of resonant driving. A large deviation will lead to a low resolution picture of synchronized pattern as shown in fig. 4(b), while a small deviation of stored eigenfrequencies recovers a higher resolution pattern shown in fig. 4(d). This phenomenon is very similar to our memory in that a larger error will decrease the accuracy of memory and fail an effective information recall. Therefore, the memory needs to be trained by decreasing the deviations of information (eigenfrequency) stored in the neuron molecules. Furthermore, if the neural network is stimulated by different types of stimulus, different synchronized patterns corresponding to different resonant frequencies will be retrieved. Therefore, different information can be stored in the neurons characterized by different frequency

channels and the storage capacity of information in a network is determined by the frequency discrimination of the network. If the stimuli frequencies are similar, mixing pictures of different resonant patterns will be simultaneously retrieved from the network, which corresponds to another important characteristic of our brain to enable imaginations of similar objects in our mind.

Summary. – In this article, the resonant synchronization of a well-connected network based on a modified Kuramoto model is investigated. Although the model to simulate memory is very rough, it seems to provide an alternative way to reveal the mechanism of information searching in the human brain. Physically, the stimuli from our sensory organs will construct inhomogeneous neuronal networks in our brain with different dynamical characteristics of neurons (maybe due to different molecular structures formed by different stimulus dynamics), whose responsive properties we identify here are their firing frequencies of electrical pulsing. Different frequencies represent different kinds of information stored in the neuronal network. We simulate the dynamical correlations in critical KO networks and found synchronized patterns of KOs with similar eigenfrequencies emerged in inhomogeneous KO networks by resonant driving. This result shows that there exists an enhancement of synchronized motion across the network induced by the resonant driving even to ONE node of the network, just like memory recall of our brain to get all the resonant (similar) information by a certain stimulus. However, the sensitivity and robustness of this effect should be strictly supported by two properties of the network: high connectivity and criticality. Only in a well-connected critical network, the KOs (nodes) whose frequencies coincide with the driving frequency can be activated from a random background and then synchronized together. For other types of network, the amplitude of the node driving will decrease exponentially with the distance [14] and the resonant synchronization of pulsing cannot be activated across the whole network.

As there are many different types of memories in our brain, the light, the sound or the pressure ones, etc., therefore the frequency encoding is only one possible way to store information in our brain network. However, our study suggests that the other information can also be selected and extracted by different electric stimuli from different sources with different resonant channels, and all the irrelevant information (off-resonant signals) cannot be activated by the driving signal, and, consequently, will be suppressed by a positive feedback of resonant synchronized behavior of activated ones. The results indicate that the resonant synchronization of retrieving information in a critical network is an efficient information searching mechanism and, basically, as it is a fundamental and universal phenomenon in physics, which can hopefully be applied to many other fields for resonant information retrieval in the critical networks.

* * *

We would like to thank Bryan C. Daniels for his original Fortran codes of Kuramoto model with Gaussian noises. This work was supported by the National Natural Science Foundation of China for emergency management project (Grant Nos. 11447025, 11847308).

REFERENCES

[1] Battaglia F. P. and Treves A., *Phys. Rev. E*, **58** (1998) 7738.
[2] Colman E. R. and Vukadinović Greetham D., *Phys. Rev. E*, **92** (2015) 012817.
[3] Kapelko V. V. and Linkevich A. D., *Phys. Rev. E*, **54** (1996) 2802.
[4] Comte J. C., Ravassard P. and Salin P. A., *Phys. Rev. E*, **73** (2006) 056127.
[5] Bennett M. V. and Zukin R., *Neuron*, **41** (2004) 495.
[6] Li Y., Schmid G., Hänggi P. and Schimansky-Geier L., *Phys. Rev. E*, **82** (2010) 061907.
[7] Deco G., Jirsa V. K., Robinson P. A., Breakspear M. and Friston K., *Pub. Lib. Sci. Comput., Biol.*, **4** (2008) 1.
[8] Breakspear M., *Nat. Rev. Neurosci.*, **20** (2017) 340.
[9] Rossoni E., Chen Y., Ding M. and Feng J., *Phys. Rev. E*, **71** (2005) 061904.
[10] Robinson P. A., Rennie C. J. and Rowe D. L., *Phys. Rev. E*, **65** (2002) 041924.
[11] Tass P. A., Fieseler T., Dammers J., Dolan K., Morosan P., Majtanik M., Boers F., Muren A., Zilles K. and Fink G. R., *Phys. Rev. Lett.*, **90** (2003) 088101.
[12] Strogatz S. H., *Physica D*, **143** (2000) 1.
[13] Kuramoto Y., *Chemical Oscillations, Waves, and Turbulence* (Springer, Berlin) 1984.
[14] Zanette D. H., *Eur. Phys. J. B*, **43** (2005) 97.
[15] Chen T., Liu X. and Lu W., *IEEE Trans. Circ. Syst. I. Regul. Pap.*, **54** (2007) 1317.
[16] Cumin D. and Unsworth C., *Physica D*, **226** (2007) 181.
[17] Batista C. A. S., Lameu E. L., Batista A. M., Lopes S. R., Pereira T., Zamora-López G., Kurths J. and Viana R. L., *Phys. Rev. E*, **86** (2012) 016211.
[18] Takahashi Y. K., Kori H. and Masuda N., *Phys. Rev. E*, **79** (2009) 051904.
[19] Nordenfelt A., Used J. and Sanjuán M. A. F., *Phys. Rev. E*, **87** (2013) 052903.
[20] Mofakham S., Fink C. G., Booth V. and Zochowski M. R., *Phys. Rev. E*, **94** (2016) 042427.
[21] Pikovsky A., Rosenblum M. and Kurths J., *Synchronization: A Universal Concept in Nonlinear Sciences* (Cambridge University Press) 2001.
[22] Amitai E., Lörch N., Nunnenkamp A., Walter S. and Bruder C., *Phys. Rev. A*, **95** (2017) 053858.
[23] Sompolinsky H., Golomb D. and Kleinfeld D., *Phys. Rev. A*, **43** (1991) 6990.
[24] Cassidy M., Mazzone P., Oliviero A., Insola A., Tonali P., Lazzaro V. D. and Brown P., *Brain*, **125** (2002) 1235.

[25] Klimesch W., *Int. J. Psychophysiol.*, **24** (1996) 61.
[26] Abáolo D., Hornero R., Gómez C., García M. and López M., *Med. Eng. Phys.*, **28** (2006) 315.
[27] Mormann F., Lehnertz K., David P. and Elger C. E., *Physica D*, **144** (2000) 358.
[28] Percha B., Dzakpasu R., Żochowski M. and Parent J., *Phys. Rev. E*, **72** (2005) 031909.
[29] O'Connor S. C. and Robinson P. A., *Phys. Rev. E*, **70** (2004) 011911.
[30] Jampa M. P. K., Sonawane A. R., Gade P. M. and Sinha S., *Phys. Rev. E*, **75** (2007) 026215.
[31] Sakaguchi H., *Prog. Theor. Phys.*, **79** (1988) 39.
[32] Maccone L., Bruss D. and Macchiavello C., *Phys. Rev. Lett.*, **114** (2015) 130401.
[33] Herculano-Houzel S., *Front. Hum. Neurosci.* **3** (2009) 31.
[34] Wang S.-J., Xu X.-J., Wu Z.-X. and Wang Y.-H., *Phys. Rev. E*, **74** (2006) 041915.
[35] Hodgkin A. L. and Huxley A. F., *J. Physiol.*, **117** (1952) 500.
[36] Maksimenko V. A., Runnova A. E., Frolov N. S., Makarov V. V., Nedaivozov V., Koronovskii A. A., Pisarchik A. and Hramov A. E., *Phys. Rev. E*, **97** (2018) 052405.